

Chemical Unfolding of Enolase from *Saccharomyces cerevisiae* Exhibits a Three-State Model

Dénison S. Sánchez-Miguel · Jahir Romero-Jiménez ·
César A. Reyes-López · Ana Lilia Cabrera-Ávila ·
Normande Carrillo-Ibarra · Claudia G. Benítez-Cardoza

Published online: 19 November 2009
© Springer Science+Business Media, LLC 2009

Abstract Enolase is a multifunctional protein that participates in glycolysis and gluconeogenesis and can act as a plasminogen receptor on the cell surface of several organisms, among other functions. Despite its participation in a variety of biological and pathophysiological processes, its stability and folding/unfolding reaction have not been fully explored. In this paper we present, the urea and GdnHCl-induced denaturation of enolase studied by means of fluorescence and circular dichroism spectroscopies. We found that enolase unfolds through a highly reversible pathway, populating a stable intermediate species in a range of experimental conditions. The refolding reaction also exhibits an intermediate state that might have a slightly more compact conformation compared to the unfolding intermediate. The thermodynamic parameters associated with the unfolding reaction are presented and discussed.

Keywords Unfolding · Reversibility · Protein stability · Fluorescence spectrum · Intermediate species · Circular dichroism

Abbreviations

TRIS TRIS(hydroxy-methyl) aminomethane
GdnHCl Guanidinium hydrochloride
SCM Spectral center of mass

CD Circular dichroism
SASA Solvent-accessible surface area

1 Introduction

Enolase catalyses the reversible dehydration of D-2-phosphoglycerate (PGA) to phosphoenolpyruvate (PEP) in glycolysis, and the reverse reaction in gluconeogenesis. In addition to its innate glycolytic function, enolase plays an important role in several biological and pathophysiological processes. It has been identified as a heat-shock protein, and that it can bind to cytoskeletal and chromatin structures, indicating its possible participation in transcription [29]. Moreover, anti-enolase antibodies have been detected in a variety of autoimmune diseases [1–3, 12, 19, 23, 26, 30, 32–34]. Enolase has been observed on the cell surface of a variety of hematopoietic, epithelial and endothelial cells, serving as a plasminogen receptor, suggesting that this enzyme participates in the intravascular and pericellular fibrinolytic system as well [29 and references therein]. Also, this molecule has been considered to be a diagnostic tumor marker [13]. A recent work revealed the existence of a regulatory circuit between c-myc, MBP-1 and enolase, which connects cellular energy metabolism and proliferation [38]. What's more, the enolase differential expression in mammalian tissues suggests that enolase could play an important sensor or regulator role in multiple stress situations [31].

Structurally, enolase is the archetypal member of the enolase superfamily. As is the case with the rest of the members, this enzyme shows an N-terminal $\alpha+\beta$ capping domain and a C-terminal $(\alpha/\beta)_8$ modified TIM-barrel domain [41]. The active site cavity is at the C-terminal end of the barrel. Both domains include loops that fold over the active site when the substrate is bound. For most of the

D. S. Sánchez-Miguel · J. Romero-Jiménez ·
C. A. Reyes-López · A. L. Cabrera-Ávila · N. Carrillo-Ibarra ·
C. G. Benítez-Cardoza (✉)
Laboratorio de Investigación Bioquímica, Programa
Institucional en Biomedicina Molecular, Sección de Estudios de
Posgrado, ENMyH-Instituto Politécnico Nacional,
Guillermo Massieu Helguera No. 239, La Escalera
Ticomán, DF 07320, Mexico
e-mail: beni1972uk@gmail.com

species, enolase has been described as a homodimeric protein, with the exception of enolases from some thermophilic bacteria [8, 37, 40] and from *Streptococcus pneumoniae* [15] that have been described as homo-octameric.

The unfolding reaction of enolase had been studied in the past using heat, pressure, urea or guanidine chloride, changes of pH or a combination of these. Most of these studies have been centered on yeast enolase. In general, it has been found that divalent cations such as magnesium and manganese are capable of stabilizing the enzyme, as well as substrate, substrate analogs, and some other ions such as acetate [6, 7, 11, 14, 16, 17, 35, 45, 46]. Some studies have suggested that unfolding might populate at least one intermediate species, or should be accompanied by dissociation of dimers into monomers [42]. However, in several cases, these intermediates have not been demonstrated under the experimental conditions tested.

We report here further analysis of the urea- and GdnHCl-induced unfolding of yeast enolase using probes for secondary and tertiary structure. Results demonstrate that unfolding of yeast enolase occurs by a three-step process that comprises a stable intermediate under a wide range of experimental conditions. The thermodynamic parameters associated with the unfolding process, at different experimental conditions, are presented.

2 Materials and Methods

2.1 Materials

Yeast enolase was purchased from Sigma and was used without any further purification. Concentrations of protein solutions were determined from their absorbencies at 280 nm, using the absorption coefficient reported for enolase ($\epsilon = 0.895 \text{ mg mL}^{-1}$) [5]. The studies were carried out in three different buffers: potassium phosphate, TRIS-acetate, or TRIS-HCl; all of them at a 50 mM concentration and pH 7.4 (at 25 °C). Some experiments were complemented with 2 mM MgSO_4 as indicated. All reactants were analytical grade. The water used was distilled and deionized. In all cases, curves are reported as the average of at least two independent experiments. All the assays were carried out using the same lot of protein. Additionally, in order to verify the data, the experiments were repeated using a different protein lot.

2.2 Activity Assays

The enolase activity was measured by coupling its reaction to pyruvate kinase and lactate dehydrogenase by following the decrease of NADH absorbance at 340 nm using a Beckman DU-650 spectrophotometer. This assay was

performed at 25 °C in a 0.1 mL reaction mixture containing 0.05 M potassium phosphate or TRIS-acetate, or TRIS-HCl buffer, pH 7.4, 1.9 mM PGA, 1.3 mM ADP, 0.12 mM NADH, and 25 μM MgSO_4 and 100 mM KCl. The auxiliary enzymes were used at final activities of 2.3 and 3.3 U mL^{-1} , respectively. One activity unit is defined as the conversion of 1.0 μmol of PGA to PEP per minute.

2.3 CD Spectra

CD measurements were performed using a JASCO J-715 spectropolarimeter (Jasco Inc., Easton, MD) equipped with a PTC-348WI Peltier-type cell holder for temperature control and magnetic stirring. CD spectra were recorded using 1.0 cm path-length cells from 200 to 250 nm at 25 °C. Ellipticities are reported as mean residue ellipticity $[\theta]$.

2.4 Fluorescence

Fluorescence spectra were obtained using an LS-55 Spectrofluorometer (Perkin-Elmer), equipped with a water-jacketed cell holder for temperature control. All the experiments were performed using cells with a path-length of 1.0 cm, at 25 °C. The excitation wavelength was 280 nm and the emission spectra were collected from 320 to 400 nm. The fluorescence spectral centre of mass (SCM) was calculated from the fluorescence intensity data (I_λ), obtained at different wavelengths (λ) from 320 to 400 nm, using the equation [25]:

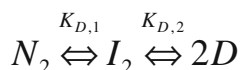
$$\text{SCM} = \frac{\sum (\lambda \times I_\lambda)}{\sum I_\lambda} \quad (1)$$

2.5 Urea and GdnHCl Induced Unfolding/Refolding of Enolase

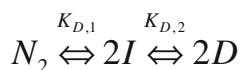
Stock solutions of protein were prepared by diluting lyophilized enolase in each of the three buffers. Afterwards, these solutions were used to prepare 10 $\mu\text{g mL}^{-1}$ enolase solutions at different urea and GdnHCl concentrations, ranging from 0 to 7.5 M and from 0 to 6 M, respectively, with 0.1 M intervals. The samples were incubated at 25 °C for 24, 48, 72, 96 and 164 h. A similar procedure was employed in preparing the solution for refolding experiments, with the exception that the protein was first denatured by adding a 10 M urea or 8.0 M GdnHCl solutions, incubated for 24 h, and then diluted up to 10 $\mu\text{g mL}^{-1}$ with the appropriate buffer. Urea and GdnHCl concentrations were determined by refractive index and the following equations:

$$[\text{urea}] = 117.66(\Delta N) + 29.753(\Delta N)^2 - 185.56(\Delta N)^3 \quad (2)$$

or



Scheme 1 Three-state dimer model involving a dimeric intermediate



Scheme 2 Three-state dimer model involving a monomeric intermediate

$$[\text{GdnHCl}] = 57.147(\Delta N) + 36.68(\Delta N)^2 - 91.60(\Delta N)^3 \tag{3}$$

respectively, where ΔN is the difference between the refractive index of a urea or GdnHCl solution and that of the respective buffer [27, 44].

2.6 Data Analysis

Three-state dimer models involving either a dimeric (Scheme 1) or a monomeric (Scheme 2) intermediate were applied to the enolase unfolding data, where N_2 , I , I_2 and D are native, monomeric intermediate, dimeric intermediate and unfolded protein, respectively [20, 36].

For a three-state model involving a dimeric intermediate (Scheme 1) the equilibrium constants for the first ($K_{D,1}$) and second ($K_{D,2}$) transitions can be defined, respectively, as:

$$K_{D,1} = \frac{[I_2]}{[N_2]} \tag{4}$$

$$K_{D,2} = \frac{[D]^2}{[I_2]} \tag{5}$$

The total protein concentration in terms of monomer is $P_t = 2[N_2] + 2[I_2] + [D]$, and the sum of the fractions of individual species is equal to $f_{N_2} + f_{I_2} + f_D = 1$, where f_{N_2} , f_{I_2} and f_D are the molar fractions of the protein present in native, intermediate and denatured states, respectively. Combining these relationships we obtain:

$$K_{D,1} = \frac{f_{I_2}}{f_{N_2}} \tag{6}$$

$$K_{D,2} = \frac{2P_t f_D^2}{f_{I_2}} \tag{7}$$

f_{N_2} , and f_{I_2} can be defined only in terms of f_D , $K_{D,1}$, $K_{D,2}$ and P_t . f_D can be expressed as a function of $K_{D,1}$, $K_{D,2}$ and P_t

$$f_D = \frac{-K_{D,1}K_{D,2} + \sqrt{(K_{D,1}K_{D,2})^2 + 8(1+K_{D,1})(K_{D,1}K_{D,2})P_t}}{4P_t(1+K_{D,1})} \tag{8}$$

In a three-state model the relative spectroscopic signal (y), becomes:

$$Y = y_{N_2}f_{N_2} + y_{I_2}f_{I_2} + y_Df_D \tag{9}$$

where y_{N_2} , y_{I_2} and y_D are the spectroscopic signals for the native, intermediate and denatured states. The fitting equation is obtained by substituting Eqs. (6) and (7) in the Eq. (9):

$$y = y_{N_2} \left(\frac{2P_t f_D^2}{K_{D,1}K_{D,2}} \right) + y_{I_2} \left(\frac{2P_t f_D^2}{K_{D,2}} \right) + y_D f_D \tag{10}$$

Free energy of unfolding and dissociation can be estimated using:

$$-\Delta G_{D,1} = -RT \ln K_{D,1} \tag{11}$$

$$-\Delta G_{D,2} = -RT \ln K_{D,2} \tag{12}$$

Considering the linear free energy model, which states that the free energy of unfolding varies linearly with concentration of denaturant [28, 39]:

$$-\Delta G_{D,1} = \Delta G_{D,1}^{H_2O} - m_1[\text{denaturant}] \tag{13}$$

$$-\Delta G_{D,2} = \Delta G_{D,2}^{H_2O} - m_2[\text{denaturant}] \tag{14}$$

where $\Delta G_{D,1}^{H_2O}$, $\Delta G_{D,2}^{H_2O}$ are the free energy of unfolding and dissociation in the absence of denaturant, m_1 and m_2 are the constants of proportionality relating to the solvent exposure difference between native and intermediate or intermediate and denatured states respectively.

The total Gibbs free energy of folding ($\Delta G_{D,tot}^{H_2O}$) is the difference in free energy between the unfolded monomers and the native dimer and can be calculated from $\Delta G_{D,1}^{H_2O}$ and $\Delta G_{D,2}^{H_2O}$:

$$\Delta G_{N_2-D}^{H_2O} = \Delta G_{D,1}^{H_2O} + \Delta G_{D,2}^{H_2O} \tag{15}$$

The m_{tot} can be calculated from m_1 and m_2 :

$$m_{tot} = m_1 + m_2 \tag{16}$$

For a three state model involving a monomeric intermediate (Scheme 2), the equilibrium constants $K_{D,1}$ and $K_{D,2}$ for the dissociation and unfolding steps, and are defined as:

$$K_{D,1} = \frac{[I]^2}{[N_2]} \tag{17}$$

$$K_{D,2} = \frac{[D]}{[I]} \tag{18}$$

The total protein concentration in terms of monomer is $P_t = 2[N_2] + [I] + [D]$, and again $f_{N_2} + f_I + f_D = 1$. Combining these relationships results in:

$$K_{D,1} = \frac{2P_I f_I^2}{f_{N_2}} \quad (19)$$

$$K_{D,2} = \frac{f_D}{f_I} \quad (20)$$

f_{N_2} and f_D can be defined in terms of f_I , $K_{D,1}$, $K_{D,2}$ and P_I . f_I can be obtained using:

$$f_I = \frac{-K_{D,1}(1 - K_{D,2}) + \sqrt{K_{D,1}^2(1 + K_{D,2})^2 + 8P_I K_{D,1}}}{4P_I} \quad (21)$$

The observed value of measured “ y ” parameter is assumed to be additive, according to the following equation:

$$y = y_{N_2} f_{N_2} + y_I f_I + y_D f_D \quad (22)$$

where y_{N_2} , y_I and y_D are the characteristic values for the native, intermediate and denatured states. The fitting equation is obtained by substituting Eqs. (19) and (20) in the Eq. (21):

$$y = y_{N_2} \left(\frac{2P_I f_I^2}{K_{D,1}} \right) + y_I (f_I) + y_D (K_{D,2} f_I) \quad (23)$$

In this case, the total Gibbs free energy of folding ($\Delta G_{N_2-D}^{\text{H}_2\text{O}}$) can be calculated as:

$$\Delta G_{N_2-D}^{\text{H}_2\text{O}} = \Delta G_{D,1}^{\text{H}_2\text{O}} + 2\Delta G_{D,1}^{\text{H}_2\text{O}} \quad (24)$$

The m_{tot} can be calculated from m_1 and m_2 :

$$m_{\text{tot}} = m_1 + 2m_2 \quad (25)$$

2.7 Solvent-Accessible Surface Area and m -Value Calculations

The solvent-accessible surface area (SASA) of native dimeric enolase was calculated from the coordinates of its X-ray crystal structure (1ONE, [18]), using the web-based program GETAREA version 1.1 [10]. The SASA of the unfolded enolase was estimated using values for individual residues obtained from tripeptide studies [21]. These studies used Gly-X-Gly tripeptides as model compounds for the SASA of side chains in the unfolded state. It has been shown that the m -value of a protein is highly correlated with the Δ SASA between native and denatured states, and the following relationships have been observed for proteins [24]:

$$\text{urea} - m = 374 + (0.11) \Delta \text{SASA} \quad (26)$$

$$\text{GdnHCl} - m = 859 + (0.22) \Delta \text{SASA} \quad (27)$$

These relationships, along with the Δ SASA calculated for the yeast-enolase unfolding transition, were used to estimate the m -value associated with complete yeast-enolase unfolding from native dimer to two unfolded monomers.

3 Results

Firstly, enzymatic activity, secondary and tertiary structures, of native enolase diluted in each of the buffers used here were analyzed. Figure 1 shows emission fluorescence and CD spectra of native enolase. The spectra are superposable reflecting that neither tyrosine nor tryptophan environments nor secondary structure suffer important modifications due to the change of buffer.

Furthermore, activity assays indicated that enolase shows the same specific activity (110 U mg⁻¹) in TRIS–acetate or TRIS–HCl buffers, whereas the specific activity was diminished (70 U mg⁻¹) in phosphate buffer as expected, because phosphate group is a competitive inhibitor of enolase [43].

The unfolding of yeast enolase was investigated by monitoring the changes in the intrinsic fluorescence and circular dichroism, using GdnHCl or urea as denaturants in three different buffers. Figure 1a shows the fluorescence emission spectra of native (in 0.0 M denaturant), and denatured yeast enolase (in 7.0 M urea) in potassium phosphate, after 164 h of incubation time. This figure clearly shows a red-shift of the SCM values from 350 to approximately 357 nm, which indicates that there is an increase in the accessibility of tryptophanyl fluorophores to the solvent. Similar results were observed in the other buffers and when GdnHCl was used as denaturant. The far-UV CD spectrum of native enolase in potassium phosphate buffer displayed a double minimum around 210 and 222 nm, (Fig. 1b), consistent with the known three-dimensional structure, and with other CD spectra reported previously in the literature for enolases from different biological species. Upon complete denaturation in 7 M urea, there was a large decrease in CD signal intensity, indicating disruption of secondary structure.

3.1 Urea Induced Denaturation

The urea-induced denaturation profiles of enolase monitored by fluorescence spectroscopy either in potassium phosphate, TRIS–acetate or TRIS–HCl buffers, at different incubation times are shown in Fig. 2 (panels a, b and c respectively). The most important feature is that none of the profiles appear as single sigmoid curves. Bimodal denaturation curves are indicative of at least one intermediate. In our results the intermediate species appears in all the tested conditions, and the initial transition seems very cooperative, especially compared with the subsequent one. It is also noticeable that at concentrations between 1.0 and 4 M urea the denaturation process does not reach equilibrium or completion even at very long incubation times (almost 7 days of incubation). Particularly, fluorescence spectral-changes with time were

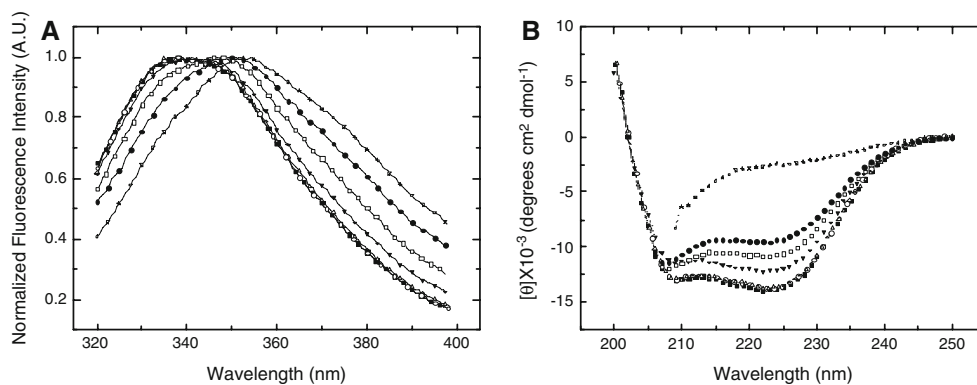


Fig. 1 Fluorescence emission (*panel A*; excitation wavelength 280 nm.) and far-UV circular dichroism (*panel B*) spectra of yeast enolase. Native yeast enolase at 25 °C was diluted ($10 \mu\text{g mL}^{-1}$) in three different buffers; potassium phosphate (*filled square*), TRIS-acetate (*open circle*) or TRIS-HCl (*open triangle*), all of them at pH 7.4. Alternatively, it was incubated for 24 h (*open square*), or 164 h

(*filled circle*), 25 °C, phosphate buffer containing 2.3 M urea, or for 164 h with 6 M urea (*star*). In order to evaluate the refolding of yeast enolase, firstly the enzyme was incubated for 24 h in potassium phosphate buffer with 10 M urea and the diluted in potassium phosphate buffer (*filled inverted triangle*)

detected between the first transition and the intermediate species zones (in all buffer solutions). From the transition curves, it is interesting to observe that the intermediate species that appears at shorter incubation times goes through structural changes that results in a conformation with different tryptophanyl environment. At higher denaturant concentrations (above 4 M urea), the fluorescence signal converges for all incubation times, with no further conformational changes, meaning that the unfolding process has reached equilibrium. For sake of comparison, the enolase unfolding transitions obtained in each of the buffers, after 164 h of incubation are shown in Fig. 3. Here, it is clear that enolase denaturation-transition profiles obtained with TRIS-HCl buffer appears at lower urea concentrations than those observed for the other two buffers. This might indicate that although the secondary and tertiary structure of enolase under all the tested conditions seem to be almost identical, the native contacts of the protein in the presence of phosphate or acetate ions, are more stable than those in TRIS-HCl. This is confirmed by the $\Delta G_{N_2-D}^{\text{H}_2\text{O}}$ values (Gibbs free energy changes, associated with the unfolding reaction in water) reported in Table 1 (see below).

Regarding the urea-induced denaturation profiles obtained in potassium phosphate and TRIS-acetate buffers, we can observe how both start at very similar urea concentrations (around 1 M), but reach different SCM values at higher urea concentrations. More precisely, the enolase-denatured state in TRIS-acetate shows a less polar tryptophan environment, compared to those obtained in the other buffers. There are at least two ways to explain this observation; a first alternative would be that the enolase-denatured states from the different buffered-solutions are indeed structurally different. A second one, would be that all the unfolded states are structurally similar, but with the

tryptophan residues having a different hydration level. The CD spectra of the denatured species in the different buffers used were almost indistinguishable, reinforcing our second alternative.

3.2 GdnHCl Induced Denaturation

The unfolding curves for yeast enolase in potassium phosphate or TRIS-HCl buffers using GdnHCl as denaturant at different incubation times are shown in Fig. 4 (panels a and b respectively). These denaturation transitions also appear as two step profiles, indicating that an intermediate species could also be present in GdnHCl-induced denaturation. In this case, completion of the reaction was reached, around 96 h of incubation time. Above 1.0 M GdnHCl the fluorescence signal converges for all incubation times. The comparison of the transition curves obtained in the two buffers is shown in Fig. 5. Similar to the results for urea-induced unfolding, yeast enolase seems to be more stable in potassium phosphate buffer than in TRIS-HCl. Also, it can be seen that the denatured state achieved in potassium phosphate buffer shows a less polar tryptophan environment, compared to that obtained in the TRIS-HCl solution. As we mentioned above, we propose that the unfolded states in both buffer solutions are structurally similar, but with the tryptophan residues having a different hydration level.

3.3 The Intermediate Species

The fluorescence emission and CD spectra of the intermediate species (in phosphate buffer, 2.3 M urea, after 24 and 164 h of incubation time) are shown in Fig. 1a, b respectively. The fluorescence emission spectrum of the

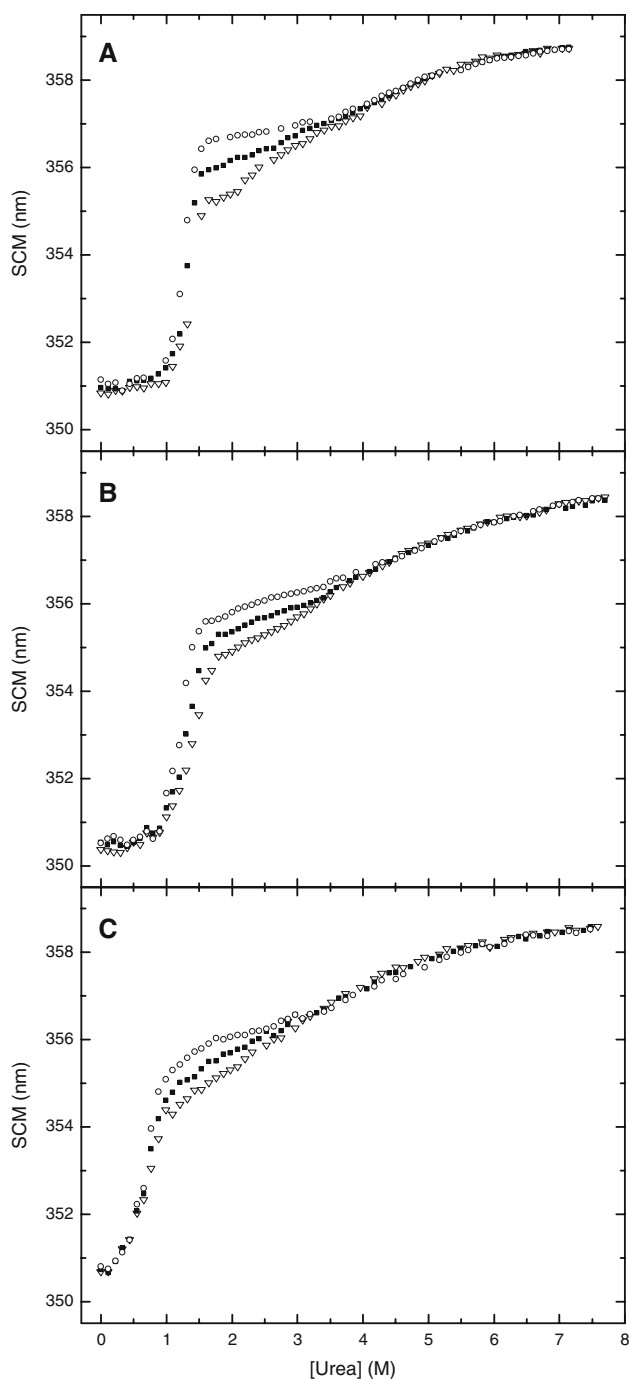


Fig. 2 Urea-induced denaturation profiles of yeast enolase monitored by fluorescence spectroscopy (samples were excited at 280 nm) in **a** potassium phosphate, **b** TRIS-acetate and **c** TRIS-HCl buffers, all of them at pH 7.4, and 25 °C. Samples were incubated for 24 (*open inverted triangle*), 72 (*filled square*) and 164 (*open circle*) h. Protein concentration was 10 $\mu\text{g mL}^{-1}$

intermediate is red shifted to longer wavelengths (Fig. 1a) than native enolase. As mentioned before, the shifting is increased at longer incubation times. This result indicates that tryptophan residues are indeed, on average, in a more polar environment in the intermediate state than in the

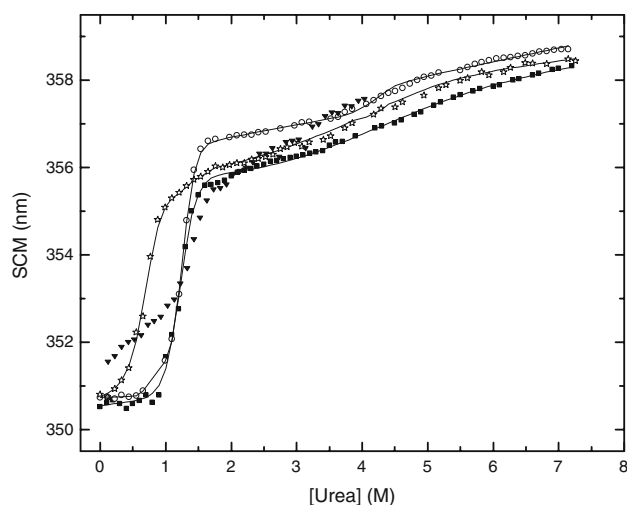


Fig. 3 Urea-induced unfolding and refolding profiles of yeast enolase monitored by fluorescence spectroscopy. Samples were incubated for 164 h in potassium phosphate (*star*), TRIS-acetate (*open circle*) and TRIS-HCl (*filled square*) buffers, all of them at pH 7.4 and 25 °C. The refolding (*filled inverted triangle*) transition was obtained as described in “Materials and Methods” section. The continuous lines represent the best fit of the unfolding curves to a three-state dimer denaturation model with a dimeric intermediate (Eq. 10)

native enzyme. Also the intermediate species shows decreased secondary structure compared to the native protein, as judged from CD spectral amplitude at 222 nm. The secondary structure is further diminished at longer incubation times. The denatured state shows a larger disruption of secondary structure with its tryptophans extensively exposed to solvent. The fluorescence emission and CD spectra in the other buffers or with GdnHCl as denaturant were not significantly different (data not shown).

3.4 Effect of Magnesium in GdnHCl Unfolding of Yeast Enolase

In previous works, it has been shown that enolase gains considerable stability in the presence of divalent cations such as Mg^{2+} or Mn^{2+} [7, 17, 46]. This was also investigated under our experimental conditions. Figure 5 shows the denaturation profiles of enolase induced by GdnHCl in phosphate buffer complemented with 2 mM MgSO_4 , in the same plot, the unfolding transition, at the same experimental conditions, but lacking Mg^{2+} is shown. From these figures, it is clear that the three-state denaturation mechanism prevails in the presence of the dimeric cation. Also, it is manifest that the unfolding curve shifts slightly to higher GdnHCl concentrations (about 0.2 M). The main difference observed between the curves with or without magnesium is that the denatured state in the presence of the divalent cation shows a less polar tryptophan environment, compared to the obtained in the absence of magnesium. CD

Table 1 Thermodynamic parameters for yeast enolase chemical denaturation

Buffer	Denaturant	ΔG_{D-1} (kcal mol ⁻¹)	m_1 (kcal mol ⁻¹ M)	ΔG_{D-2} (kcal mol ⁻¹)	m_2 (kcal mol ⁻¹ M)	^a ΔG_{D-tot} (kcal mol ⁻¹)	^b m_{tot} (kcal mol ⁻¹ M)
Model: N ₂ ↔ I ₂ ↔ 2U							
Phosphate	Urea	8.1 (0.3)	6.5 (0.2)	19.1 (1.0)	2.1 (0.2)	27.2	8.6
TRIS-HCl	Urea	3.1 (0.1)	4.2 (0.2)	17.2 (0.8)	1.5 (0.2)	20.3	5.7
TRIS-Acetate	Urea	6.6 (0.3)	5.5 (0.2)	21.2 (4.1)	2.2 (0.7)	27.8	7.7
Phosphate	GdnHCl	5.3 (0.2)	14.6 (0.2)	16.9 (0.4)	2.8 (0.2)	22.2	17.4
TRIS-HCl	GdnHCl	4.9 (0.4)	25.2 (2.0)	16.1 (0.7)	2.6 (0.3)	21.0	27.8
Phosphate + MgSO ₄	GdnHCl	6.8 (0.1)	12.7 (0.1)	23.2 (1.8)	3.7 (0.7)	30.0	16.4
Buffer	Denaturant	ΔG_1 (kcal mol ⁻¹)	m_1 (kcal mol ⁻¹ M)	ΔG_2 (kcal mol ⁻¹)	m_2 (kcal mol ⁻¹ M)	^c ΔG_{D-tot} (kcal mol ⁻¹)	^d m_{tot} (kcal mol ⁻¹ M)
Model: N ₂ ↔ 2I ↔ 2U							
Phosphate	Urea	11.0 (1.8)	8.2 (0.8)	13.2 (0.5)	3.0 (0.1)	37.4	14.2
TRIS-HCl	Urea	4.4 (0.2)	5.4 (0.3)	8.7 (0.4)	2.0 (0.1)	21.8	9.4
TRIS-Acetate	Urea	8.9 (0.3)	6.8 (0.3)	12.6 (0.3)	2.8 (1.4)	34.1	12.4
Phosphate	GdnHCl	5.7 (0.7)	17.8 (2.3)	7.2 (0.4)	3.4 (0.2)	20.1	24.6
TRIS-HCl	GdnHCl	6.9 (0.8)	36.3 (4.3)	7.4 (0.8)	1.6 (0.3)	21.7	39.5
Phosphate + MgSO ₄	GdnHCl	8.8 (0.1)	13.2 (0.1)	15.2 (1.8)	4.2 (0.7)	39.2	21.6

Measurements were made at 25 °C and pH 7.4. Global analysis was performed with the non-linear, least-squares fitting program Origin, version 7.0. Standard deviations are indicated in parentheses

^a Calculated according to Eq. 15

^b Estimated using Eq. 16

^c Calculated according to Eq. 24

^d Estimated using Eq. 25

spectra analysis revealed that the denatured state obtained in the presence of the divalent cation seems to be more ordered than in the absence of Mg²⁺ (data not shown).

3.5 Reversibility of the Unfolding Reaction

The fluorescence-emission and CD spectra upon renaturation are shown in Fig. 1 and the refolding profiles are shown in Figs. 3 and 5, respectively, both in potassium phosphate buffer. From these figures, and from the recovery of enzyme activity, we conclude that enolase is capable of recovering about 80–85% of its native structure after the urea or GdnHCl-induced unfolding. This reveals that the reactions leading to irreversibility are not so significant, even at very long exposure times to 10 M urea. Commonly, irreversibility is attributed to unspecific aggregation of the denatured conformations that expose hydrophobic surfaces. In our studies, no aggregation was detected, probably because urea or GdnHCl and low protein concentrations could have prevented it. Nonetheless, the unfolding/refolding curves of yeast enolase were not identical. This result suggests that the unfolding/refolding process is out of equilibrium or kinetically controlled. It is interesting that the refolding intermediate state shows slightly lower SCM values than the unfolding intermediate state, suggesting

that it might be a more compact conformation. Another interesting observation is that the refolding reaction occurs faster (24 h incubation) than the unfolding process. This might imply that the refolding reaction might have smaller kinetic barriers than the unfolding process.

3.6 Thermodynamic Parameters of the Unfolding/Refolding Reaction of Enolase

In order to obtain the $\Delta G_{N_2-D}^{H_2O}$ values associated with the unfolding/refolding reaction of yeast enolase, we assumed that the reaction was near the equilibrium. This assumption was supported on two experimental observations. One is the high reversibility observed in the denaturation reaction (about 80–85%). The other one was that fluorescence emission and CD signals changed less significantly when increasing incubation times, indicating that the unfolding reaction was close to completion. Therefore, we selected the transition curves obtained at 164 and 96 h (urea and GdnHCl experiments, respectively) to calculate the thermodynamic parameters. It should be considered that the parameters presented here are apparent and must be taken as estimations. According to the experimental data, the unfolding transitions appeared as two-step processes. Thus, three-state dimer models involving either a dimeric

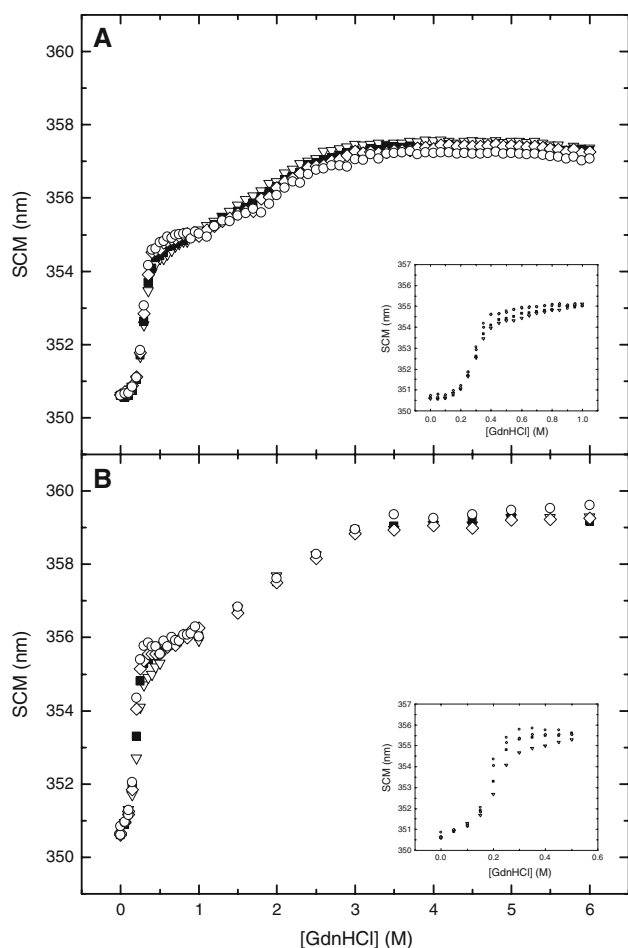


Fig. 4 GdnHCl-induced denaturation profiles of yeast enolase monitored by fluorescence spectroscopy (samples were excited at 280 nm) in **a** potassium phosphate, and **b** TRIS–HCl buffers, at pH 7.4, and 25 °C. Samples were incubated for 2 (*open inverted triangle*), 24 (*filled square*), 48 (*diamond*) and 96 (*open circle*) h. The insets represent the same set of data, for the first transition and intermediate zones. Protein concentration was 10 $\mu\text{g mL}^{-1}$

(Scheme 1) or a monomeric (Scheme 2) intermediate were applied to the enolase unfolding data. Both models could fit the data; however, the better fit to the data, in all experimental conditions, was achieved using a three-state dimer denaturation model with a dimeric intermediate. The thermodynamic parameters obtained with both models are shown in Table I. The parameters in this Table confirm that enolase seems to be more stable when diluted in TRIS–acetate or potassium phosphate buffer, compared to TRIS–HCl buffer, as presumed from the unfolding profiles.

3.7 Relating m -Values and the Change in Solvent Accessible Surface Area

The change in solvent-accessible surface area (ΔSASA) upon unfolding is strongly correlated with the m -value of a protein. We were able to estimate urea- m and GdnHCl- m

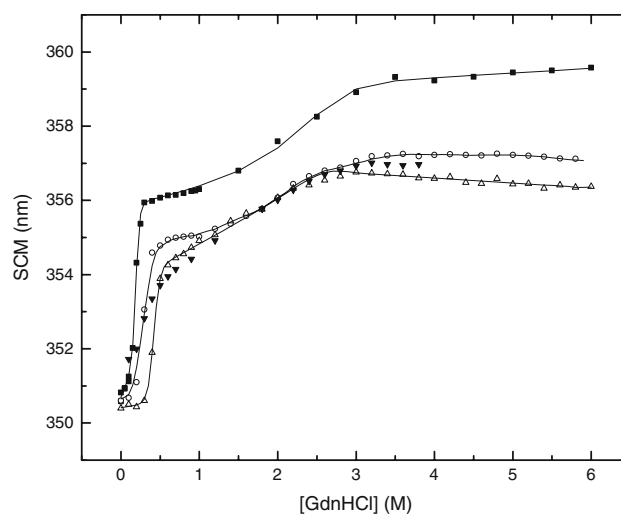


Fig. 5 GdnHCl-induced unfolding and refolding profiles of yeast enolase monitored by fluorescence spectroscopy. Samples were incubated for 96 h in potassium phosphate (*open circle*), potassium phosphate complemented with 2 mM MgSO_4 (*open triangle*) and TRIS–HCl (*filled square*) buffers, all of them at pH 7.4 and 25 °C. The refolding (*filled inverted triangle*) transition was obtained as explained in Materials and Methods section. Data points were fitted to a three-state dimer denaturation model involving a dimeric intermediate (Eq. 10, smooth lines)

values after evaluating ΔSASA , using Eqs. 26 and 27 respectively (Table 2; urea- $m = 9.1 \text{ kcal mol}^{-1} \text{ M}^{-1}$ and GdnHCl- $m = 19.2 \text{ kcal mol}^{-1} \text{ M}^{-1}$). They are roughly in good agreement with the m_{tot} values shown in Table 1 (urea: 5.7–8.6 $\text{kcal mol}^{-1} \text{ M}^{-1}$; 17.4–31.9 $\text{kcal mol}^{-1} \text{ M}^{-1}$; assuming a dimeric intermediate denaturation model).

4 Discussion

4.1 Unfolding Mechanism of Yeast Enolase

For dimeric proteins, the overall unfolding reaction must start with the folded dimer (N_2) and end with two unfolded monomers ($2D$). When the unfolding reaction involves at least one intermediate, it could be either dimeric (Scheme 1) or monomeric (Scheme 2). In these instances, one expects biphasic unfolding curves and/or non-superimposable transitions if the spectral probes used are differentially sensitive to the various species. As a general trend, for dimeric proteins a monomeric intermediate becomes more populated as protein concentration is decreased whereas a dimeric intermediate becomes more populated as protein concentration is increased [20, 36].

In the case of enolase, previous studies have reported that the folding/unfolding pathway of enolase might be a multistep process. For example, Huang and Dong [14] presented the enolase GdnHCl-induced unfolding in the

Table 2 Changes in SASA for yeast enolase upon unfolding, along with estimated m -values

^a Native dimer (N ₂) SASA (Å ²)	^b SASA estimate for unfolded protein (Å ²)	^c ΔSASA for unfolding	^d m -value estimate for unfolding N ₂ ↔2D (kcal mol ⁻¹ M ⁻¹)
28433	107655	79221	Urea- m =9.1 GdnHCl- m =19.2

^a Calculated using the web-based program GETAREA, version 1.1 [10]

^b Calculated using values from tripeptide studies [21]

^c ΔSASA for unfolding = (SASA unfolded protein, 2D)–(SASA folded protein, N₂)

^d Estimated using Eqs. (26 and 27), correlation equations given by Myers et al. [24]

absence of divalent cations. Most of the experimental conditions they used were similar to some of those used by us (50 mM potassium phosphate buffer, pH 7.2, 25 °C), except for the protein concentration. They used 20 mg mL⁻¹, whereas we used only 10 μg mL⁻¹ *i.e.* 2000 times more than us. Huang and Dong [14] detected the first changes on the infrared spectra of enolase from a 0.4 M GdnHCl concentration, evidenced by the loss of the α -helix and β -sheet structures. They observed that the fully unfolded state was reached at 1.6 M. They also observed a significant amount of intermolecular β -sheet aggregate between 0.6 and 1.0 M GdnHCl concentrations, which disappeared as the denaturant concentration increased. They described the GdnHCl-unfolded state as a heterogeneous ensemble of turns, helix/loops, and random structures, which continues to change at higher denaturant concentrations. Although they were not able to detect any intermediate species, they concluded that GdnHCl-induced equilibrium unfolding of yeast enolase is a multi-state event due to the lack of a clearly defined isosbestic point in the overlaid spectra of unfolding. Also, the thermal denaturation of yeast enolase studied by differential scanning calorimetry was described as a multi-step process where the enzyme dissociates before denaturing [7]. Furthermore, the GdnHCl-induced denaturation of enolase from *Plasmodium falciparum* was described as a three-state model, with dissociation of the dimer into monomers occurring previously to the opening of the molecule [42].

In this work, we were able to detect an intermediate species at all experimental conditions tested. Some attempts to investigate the oligomeric state of the intermediate species were carried out, but unfortunately, the interpretation of the data was difficult because, as was noted before, the spectroscopic signals vary significantly with incubation time. Therefore, we were not able to acquire convincing evidence of the oligomeric state of the intermediate species. Nevertheless, considering that experimental data were better fit with a dimeric-intermediate model, we can assume that the three-state model involving a dimeric intermediate could be the most reliable (assuming that the denaturation pathway does not change with buffer).

According to the literature, dimeric intermediates tend to be formed by proteins that have large subunits (chain lengths >250 amino acids) compared to those that form monomeric intermediates (chain lengths between 100 and 250 amino acids) [36]. Proteins forming dimeric intermediates generally have dimer interface areas that are larger than 1,500 Å², and may consist of two or more domains per monomer [9]. Enolase fulfils all of these characteristics, supporting our conclusion. However, more detailed studies are necessary in order to verify the oligomeric state of the intermediate species.

4.2 Overall Stability of Yeast Enolase

Assuming that yeast enolase unfolds via a three-state model involving dimeric intermediate species, $\Delta G_{N_2-D}^{H_2O}$ varies from 20.3 to 27.8 kcal mol⁻¹. Differences in enolase stability are observed in different buffer solutions, being more stable in phosphate or TRIS–acetate buffers than in TRIS–HCl solution. Previous studies have demonstrated that enzymes that interact with phosphate containing substrates are stabilized by this ion [22]. Also calorimetric studies have demonstrated that acetate ion stabilizes yeast enolase [7], whereas potassium chloride has been demonstrated to destabilize the enolase conformation [4, 11].

The total Gibbs free energy of unfolding for dimers ranges from 16 to 80 kcal (mol monomer)⁻¹. This means that the total Gibbs free energy of unfolding of yeast enolase is within the average for dimeric proteins. Nevertheless, considering a per residue value (0.05–0.06 kcal mol residue⁻¹), yeast enolase is a less stable protein when compared with other dimeric proteins with α/β structure and that unfold through monomeric or dimeric intermediates (0.07–0.25 kcal mol residue⁻¹) at the conditions tested here [36 and references cited therein].

We have established conditions that allow a more extensive investigation of the conformational stability of enolase. The existence of a stable intermediate under a wide range of conditions brings about the necessity to further investigate the stability and kinetics of the folding/unfolding mechanism of this enzyme.

Acknowledgments We are very thankful with Dr. Andrés Hernández Arana for the use of the circular dichroism spectrometer. NCI was supported by a fellowship from CONACyT (204849) and from the Instituto Politécnico Nacional with a PIFI-IPN student grant. This work was supported by grants from TWAS (04-352 RG/BIO/LA), CONACyT (45990), and SIP-IPN (20080356, 20091074).

References

- Adamus G, Amundson D, Seigel GM, Machnicki M (1998) *J Autoimmunol* 11:671–677
- Adamus G, Aptsiauri N, Guy J, Heckenlively J, Flannery J, Hargrave PA (1996) *Clin Immunol Immunopathol* 78:120–129
- Akisawa N, Maeda T, Iwasaki S, Onishi S (1997) *J Hepatol* 26:845–851
- Brewer JM (1969) *Arch Biochem Biophys* 134:59–66
- Brewer JM, Faini GJ, Wu CA, Goss LP, Carreira LA, Wojcik R (1978) In: Catsim poolas N (ed) *Physical aspects of protein interactions*. Elsevier, North-Holland, p 57278
- Brewer JM, Glover CVC, Holland MJ, Lebioda L (1997) *Biochim Biophys Acta* 1340:88–96
- Brewer JM, Wampler JE (2001) *Inter J Biol Macromol* 28:213–218
- Brown CK, Kuhlman PL, Mattingly S, Slaters K, Calie PJ, Farrar WW (1998) *J Protein Chem* 17:855–866
- Doyle SM, Braswell EH, Teschke CM (2000) *Biochem* 39:11667–11676
- Fraczkiewicz R, Braun W (1998) *J Comp Chem* 19:319–333
- Gawronski TH, Westhead EW (1969) *Biochem* 8:4261–4270
- Gitlits VM, Sentry JW, Matthew MLSM, Smith AI, Toh BH (1997) *Immunol* 92:362–368
- He P, Naka T, Serada S, Fujimoto M, Tanaka T, Hashimoto S, Shima Y, Yamadori T, Suzuki H, Hirashima T, Matsui K, Shiono H, Okumura M, Nishida T, Tachibana I, Norioka N, Norioka S, Kawase I (2007) *Cancer Sci* 98:1234–1240
- Huang P, Dong A (2003) *Spectroscopy* 17:453–467
- Kolberg J, Aase A, Bergmann S, Herstad TK, Rødal G, Frank R, Rohde M, Hammerschmidt S (2006) *Microbiol* 152:1307–1317
- Kornblatt MJ, Al-Ghanim A, Kornblatt JA (1996) *Eur J Biochem* 236:78–84
- Kornblatt MJ, Lange R, Balny C (2004) *Eur J Biochem* 271:3897–3904
- Larsen TM, Wedekind JE, Rayment I, Reed GH (1996) *Biochem* 35:4349–4356
- Lindquist S, Craig EA (1998) *Annu Rev Genet* 22:631–677
- Mallam AL, Jackson SE (2005) *J Mol Biol* 346:1409–1421
- Miller S, Janin J, Lesk AM, Chothia C (1987) *J Mol Biol* 196:641–656
- Mixcoha-Hernández E, Moreno-Vargas LM, Rojo-Domínguez A, Benítez-Cardoza CG (2007) *Protein J* 26:491–498
- Moodie FDL, Leaker B, Cambridge G, Totty NF, Segal AW (1993) *Kidney Int* 43:675–681
- Myers JK, Pace CN, Scholtz JM (1995) *Protein Sci* 4:2138–2148
- Najera H, Costas M, Fernandez-Velasco DA (2003) *Biochem J* 370:785–792
- Orth T, Kellner R, Kiekmann O, Faust J, Meyer Zum Buschenfelde K-H, Mayet W-J (1998) *Clin Exp Immunol* 112:507–515
- Nozaki Y (1972) *Methods Enzymol* 26:43–50
- Pace CN (1986) *Methods Enzymol* 131:266–280
- Pancholi V (2001) *Cell Mol Life Sci* 58:902–920
- Peterson P, Perheentupa J, Krohn KJE (1996) *Clin Diagn Lab Immunol* 3:290–294
- Petrak J, Ivanek R, Toman O, Cmejla R, Cmejlova R, Vyoral D, Zivny R, Vulpe CD (2008) *Proteom* 8:1744–1749
- Pratesi F, Moscato S, Sabbatini A, Chimentini D, Bombardieri S, Migliorini P (2000) *J Rheumatol* 27:109–115
- Rattner JB, Martin L, Waisman DM, Johnstone SA, Fritzler MJ (1991) *J Immunol* 146:2341–2344
- Roosendaal C, Zhao MH, Horst G, Lockwoods CM, Kleibeuker JH, Limburg PC (1998) *Clin Exp Immunol* 112:10–16
- Rosenberg A, Lumry R (1964) *Biochem* 3:1055–1061
- Rumfeldt JAO, Galvagnion C, Vassall KA, Meiering EM (2008) *Progress Biophys Mol Bio* 98:61–84
- Schurig H, Rutkat K, Rachel R, Jaenicke R (1995) *Protein Sci* 4:228–236
- Sedoris KC, Thomas SD, Miller DM (2007) *Biochem* 46:8659–8668
- Tanford C (1970) *Advan Protein Chem* 24:1–95
- Veronese FM, Schiavon O, Boccù E, Benassi CA, Fontana A (1984) *Int J Pept Protein Res* 24:557–562
- Vick JE, Gerlt JA (2007) *Biochem* 18:14589–14597
- Vora HK, Shaik FR, Pal-Bhowmick I, Mout R, Jarori GK (2009) *Arch Biochem Biophys* 485:128–138
- Wang T, Himoe A (1974) *J Biol Chem* 249:3895–3902
- Warren JR, Gordon JA (1966) *J Phys Chem* 70:297–300
- Westhead EW (1964) *Biochem* 3:1062–1068
- Zhao S, Choy BS, Kornblatt MJ (2008) *FEBS J* 275:97–106